ThermicVib: Enabling Dynamic Thermal Sensation with Multimodal Haptic Glove for Thermal-Responsive Interaction

Hyung Il Yi* KAIST
Hojeong Lee† KAIST
Sang Ho Yoon‡ KAIST

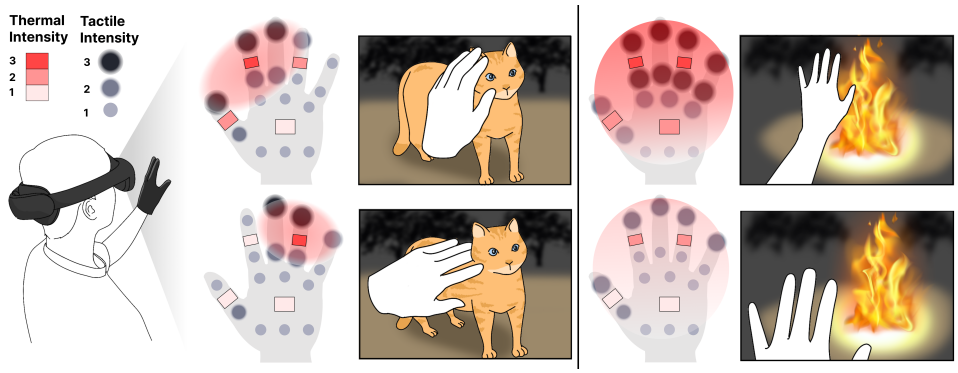

Figure 1: When the user interacts with a virtual object, either in contact or noncontact, our interface reacts to the user's action and gives adequate thermal sensation with multimodal rendering.The multimodal rendering is achieved by integration of two sensory illusions, thermal referral and vibrotactile phantom sensation.

Abstract

We propose ThermicVib, a wearable multimodal haptic glove that enhances the active perception of thermo-tactile interactions with virtual objects by integrating thermal referrals and vibrotactile phantom sensations. By fusing multimodal sensory illusions through flexible thermoelectric devices (FTED) and linear resonant actuators (LRAs), we aim to support dynamic thermal sensation adaptive to the user's action in virtual reality (VR). Here, we developed an algorithm to render a whole-hand thermal sensation while accommodating contact and noncontact heat conditions. Based on the computed heat, we propose a simultaneous thermal and tactile rendering approach to enable dynamic thermal sensation. The user study validated the capability of our interface to support various whole-hand thermal sensations.

Index Terms: Haptics, Virtual Reality, Thermal Feedback, Wearables.

1 Introduction

Thermal feedback has been recently highlighted with its capability to enhance immersive experiences in VR compared to conventional visual and tactile display-only experiences. In the real world, we naturally identify and respond to the thermal information around us, such as keeping a distance from the fire. In VR, the thermal sensation has shown improvements in spatial perception [8], and localization of spatial cue [35]. Even in the absence of providing actual thermal sensation for the user in VR, previous applications tend to visualize thermal information through color coding (e.g., red as warmth and blue as cold) [45]. This indicates the importance of keeping and alerting thermal information to users during VR interactions. To this end, recent works started to focus on providing realistic thermal sensation on the hand, which is the main interaction medium in VR.

Various heating and cooling mechanisms have been suggested to deliver realistic thermal feedback to hand. To provide distinctive thermal sensation, previous works employed a pneumatic and hydraulic approach [18], but they often required bulky hardware due to using air compressors and pumps. Researchers have focused on using a thermoelectric device (TED) that uses the Peltier effect [6] to deliver both cold and hot sensations. Even the glove using flexible thermoelectric device (FTED) with real-time feedback has been introduced [24]. Still, TED requires large power consumption if trying to cover large areas and has issues with heat dissipation when activated for a long time ($>$ 30 s). This makes it hard to apply TEDs for a whole-hand thermal sensation.

A recent approach to solving this problem is by using a thermal sensory illusion using a thermal referral [5]. In this approach, the tactile stimulus is given near the thermal stimulus to enable thermal sensation where the tactile stimulus exists [28, 41, 44]. On the other hand, researchers also employed active sensation through vibrotactile cues to stimulate thermal sensation with various haptic patterns [40]. Thus, a thermal referral approach would be a promising candidate to reduce the required number of TEDs to support whole-hand interactions. On the other hand, recent works have shown the high capability of supporting dynamic whole-hand tactile sensations [29, 42]. These works utilize the concept of vibrotactile phantom sensation, where the spatial tactile illusion can be created with the use of distant tactile stimulation [1]. This tells that vibrotactile phantom sensation, along with the thermal referral approach, has a high potential to support dynamic thermal sensation for a whole hand.

To further enhance the thermal-responsive interaction experiences, the interface should reflect the spatial thermal relationship between the users' hands and the virtual thermal objects. This means that the thermal sensation should reflect the change in distance between users' hands and the object as well as the view angle of users' hands

*e-mail: hylee0922@kaist.ac.kr
†e-mail: leeho@kaist.ac.kr
‡e-mail: sangho@kaist.ac.kr

to the object. Furthermore, various contact conditions with the hand should create a distinctive thermal sensation. For instance, warm sensations from touching a dog should be different if the user touches it with either a finger or a palm. Also, if the distant thermal object is moving, the thermal sensation should follow this change accordingly.

We believe that because thermal referral can be triggered by tactile stimuli, thermal referral can also follow the created tactile sensory illusion, which can render thermal stimuli to be felt at a specific position and can move around as well. By using the characteristics and active perception of the phantom sensation, the thermal referral can also create static, dynamic sensations and can be rendered for active perception.

In this paper, we present a thermal haptic interface that achieves interactive rendering via integrated sensory illusions of thermal referrals and vibrotactile phantom sensations. To integrate these illusions, we developed a multimodal heat rendering pipeline to coordinate the operating parameters of thermal and tactile actuators based on the relationship between the user's hands and the thermal objects. We carried out user studies to confirm the accuracy of identifying various thermal haptics patterns and the experience using our method for VR interactions. Our work showed a step toward realistic thermal sensation with the whole hand in VR. Our contributions are as follows:

- We enabled dynamic thermal sensation on the whole hand with wearable multimodal (thermal and vibrotactile) haptic interface;
- We integrated the concept of thermal referral and vibrotactile phantom sensation to support dynamic thermal sensation on the whole hand; and
- We propose a novel thermal haptic rendering pipeline to reflect the geometric relationship of the user's hands to the thermal objects.

2 Related Works

2.1 Perceptive Thermal Sensation

When rendering thermal sensation, the temperature deviation from the neutral zone and the rate of change (ROC) of temperature play crucial roles for effective thermal perception [22, 47]. The temperature range considered for the warmth perspective is defined as 32°C∼34°C to be neutral range, and 38°C∼40°C [22, 47, 50]. Although higher temperature difference provides effective warmth sensation, previous works avoided rendering extremely high temperature [40, 28] due to the heat pain threshold (45°C∼48°C) [3, 23]. In the case of attaching a heat source to the gloves or vests, however, adding an extra 10°C would be acceptable with the heat consumption from the clothing [12, 41].

ROC plays a key role in determining the effectiveness of thermal stimulation and typically operates in a range of 1°C/s∼3°C/s [46, 47]. In other work, researchers reported that ROC below 0.5°C/s or over 2°C/s does not provide meaningful thermal stimulation [30]. Furthermore, a ROC greater than 3°C/s gives discomfort to the user [47]. In our work, we set our target temperature in the range of 33°C to 45°C and selected 3 ROCs modes (Mode 1: 0.5°C/s, Mode 2 :1.5°C/s, and Mode 3: 2.5°C/s) to render the proposed thermal sensations. These temperature ranges and ROCs trigger thermal sensations safely without causing user discomfort.

2.2 Thermal Haptic Devices

Previously, various works have been proposed to enable thermal sensation including pneumatic devices with air compressors [4, 49], mid-air devices with heated airflow [40], liquid pumps with tubes [11, 32], and copper heating grids [25]. However, these approaches require large external hardware, which limits the application to wearables.

To this end, TED devices utilizing the Peltier effect have been widely adopted for wearables and consumer devices with their capability of providing rapid warm and cold sensations with small sizes [15, 33]. Still, TEDs require an additional heat sink, heat pipe, or even small fans to facilitate heat dissipation due to the high heat generation during the operation. Furthermore, TEDs can only provide thermal sensation to the installed footprint, which has limitations in wide coverage. In this work, we propose a novel thermal illusion method to mitigate the drawbacks of TEDs by minimizing the use of TEDs while maximizing thermal sensation coverage.

2.3 Thermal & Tactile Sensory Illusion

The thermal referral refers to the phenomenon where a human feels the temperature sensation on the skin in the locations where thermal and tactile stimuli are given [10]. This showed a potential of spreading thermal sensation to the skin area without placing an actual thermal source. Recent works also showed that multiple thermal stimulations without tactile stimuli enabled the thermal referral phenomenon through spatial integration [5, 17]. However, the majority of thermal sensation works focused on integrating thermal and tactile feedback with robust and effective thermal sensation performance [14, 26, 36, 39]. Similarly, vibrotactile sensory illusions such as the phantom sensation (or vibrotactile funneling illusion) and tactile apparent movement (TAM) have been proposed [1, 9]. The phantom sensation refers to the illusory tactile sensation that occurs midway between multiple distant tactile stimulations. TAM is a haptic illusion that provides a continuous motion sensation by stimulating discrete points on the skin asynchronously. Using these approaches, previous works enabled vibrotactile stimulation on wide coverage [27, 29, 42] while supporting dynamic tactile movement sensations [19]. Using vibrotactile illusions, previous work suggested that cross-modal processing supports thermal sensation with localization capability [13]. Aligned in this direction, we integrate both thermal and vibrotactile illusions to enable whole-hand thermal-responsive interactions that support localized and dynamic thermal haptic patterns.

3 ThermicVib Operating Principle

We aim to utilize the vibrotactile phantom sensation (tactile stimulus) along with thermal stimulus to enable both static and dynamic thermal sensations on the whole hand. To render an active perception of thermal sensation, we applied net heat calculation to control the intensity of tactile and thermal stimuli. Here, we followed the heat transfer model from Iman et al. [20], where we further modified the radiation formula and reflected the heat transfer with the environment. In this way, the proposed thermal haptic interface becomes capable of supporting thermal sensation for contact and noncontact conditions.

For the net heat calculation, we assumed all objects are black bodies. We considered only the heat transfer calculation between the thermal object and the interaction surface and between the interaction surface and the still-air environment. Here, we focused on heat transfer on the whole hand. For heat convection, we only considered the ambient environment. When the user interacts with the thermal object, the net heat rate change on the different areas of the hand determines the control parameters for FTEDs and LRA motors.

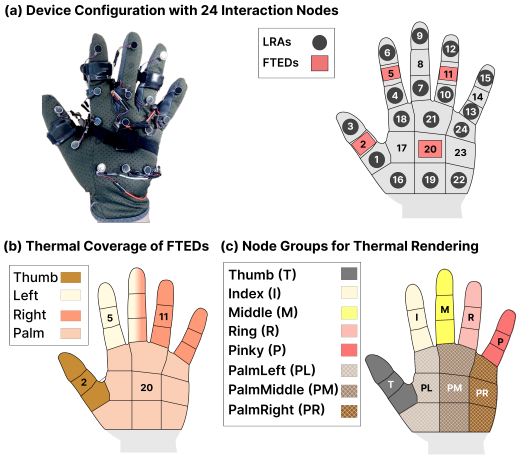

Figure 2: An interaction nodes definition for ThermicVib. (a) Locations of LRAs and FTEDs. (b) Effective thermal rendering areas by each FTED. (c) 24 interaction nodes grouped for each finger and 3 palm regions.

3.1 Thermal Interaction Nodes

To carry out net heat computation and thermal sensation, we divided the hand into 24 heat interaction nodes, including 3 on each finger and 9 on the palm (Figure 2a). The resolution was determined from the 5-location densities model [29], which set 5 haptic rendering nodes along the trajectory from each fingertip to the center of the wrist to form 21 nodes. Our work enhanced the design by covering all finger's phalange and uniformly spaced nodes on the palm. For each finger, we formed interaction nodes for each phalange to enable up and down thermal movement sensation within the finger region. For the palm, we divided the palm into uniformly spaced nodes to allow thermal movement sensation in all 2D directions. Every interaction node holds temperature information on how much intensity should be given to FTEDs (thermal stimuli) and LRAs (tactile stimuli). Each interaction node was considered as a square during computation.

For thermal rendering, we grouped the interaction nodes into 4 groups to control the intensity of 4 FTEDs (Figure 2b). To get the target temperature of each interaction node, we computed the net heat transfer rate with Eq. 1. We encompassed contact and noncontact conditions to obtain realistic thermal sensations.

$$Q_{total} = \begin{cases} Q_c - Q_{env}, & \text{if contact} \\ Q_{nc} - Q_{env}, & \text{if noncontact} \end{cases} \quad (1)$$

, where Q_{total} refers to the total net heat transfer rate in watt, Q_c represents net heat transfer rate of the contacted interaction node, Q_{nc} denotes the net heat transfer rate during noncontact neat rate of radiation from thermal object to interaction nodes, and Q_{env} is the net heat transfer rate between interaction node and ambient environment.

Contact When an interaction node is in contact with a thermal object, heat is transferred to the area through conduction (Figure 3a). Net heat transfer of area between thermal object and interaction node then is expressed as Eq. 2 when only considering x and y directions [16].

$$Q_c = k \cdot A_{int} \cdot (T_{obj} - T_{int}) \cdot (\frac{1}{\Delta x} + \frac{1}{\Delta y}) \quad (2)$$

, where k is the thermal conductivity of the hand (0.30 W/mK) [31]. Here, we assumed that interaction node is fully in contact when heat conduction occurs so

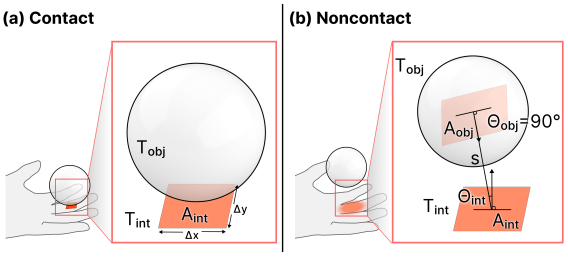

Figure 3: Overview of heat calculation for (a) contact condition and (b) noncontact condition.

cross-sectional area is set as A_{int}, which is the area of the interaction node (0.0004 m^2). This area was set to this value to utilize heat capacity in Eq. 9. T_{int} and T_{obj} represent the temperature of the interaction node and thermal object in kelvin. Δx and Δy is the width and height of the interaction node (0.02 m). ΔT is the temperature difference between the interaction node and the contacted thermal object.

Noncontact When the interaction node is not in contact, heat is transferred through radiation (Figure 3b). Net heat radiation transfer is expressed as Eq. 3.

$$Q_{nc} = \sigma \cdot A_{obj} \cdot F_{obj \to int} \cdot (T_{\text{obj}}^4 - T_{\text{int}}^4) \quad (3)$$

, where σ is the Stefan-Boltzmann constant (5.67×10^{-8} W/m^2K^4) and A_{obj} is the area of the thermal object, which is set to 1(m^2). $F_{obj \to int}$ is a view factor from the thermal object to the interaction node.

The view factor, which indicates how much radiation hits the interaction node that is emitted from a thermal object, is calculated as Eq. 4 [2].

$$F_{obj \to int} = \frac{1}{A_{obj}} \int_{A_{obj}} \int_{A_{int}} \frac{\cos\theta_{obj} \cos\theta_{int}}{\pi d^2} \, dA_{int} \, dA_{obj} \quad (4)$$

, where A_{obj} is the area of the thermal object. θ_{obj} and θ_{int} are the angles between the normal differential area of the thermal object and the interaction node. d is the distance between the two differential areas. Here, we assume that all the differential areas in the interaction node shares the same angle and distance to the thermal object. We consider that the thermal object always faces the hand, making $\cos\theta_{obj}$ always 1. Then, the view factor is simplified as Eq. 5.

$$F_{obj \to int} = A_{int} \cdot \frac{\cos\theta_{int}}{\pi d^2} \quad (5)$$

Environment For heat transfer between the environment and the interaction node, free convection and radiation is calculated as Eq. 6.

$$Q_{env} = A_{int} \cdot \sigma \, (T_{\text{int}}^4 - T_{env}^4) + h_c \cdot A_{int} \cdot \, (T_{\text{int}} - T_{env}) \quad (6)$$

, where h_c is the heat transfer coefficient of free convective flow that can be estimated as Eq. 7 [7, 38].

$$h_c = 2.44 \cdot (T_{int} - T_{env})^{0.25} \quad (7)$$

After Q_{total} has been calculated, the heat capacity of the hand is used to determine how much temperature needs to be added. Q_{total} also can be expressed as Eq. 8 [2] .

$$Q_{total} = \frac{C_{int} \cdot \Delta T_{int}}{\Delta t} \quad (8)$$

, where C_{int} is the heat capacity of the interaction node (6.3 J/K for 0.0004m^2) [37] and Δt is unit time (1 s).

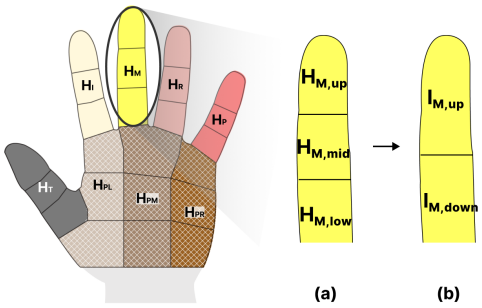

Figure 4: Heat definition of each group. (a) shows upper, middle, and lower interaction nodes that are within the group. (b) shows heat value changing to intensity ratio of up and down to determine the intensity of LRAs in tactile rendering.

Then, the amount of actual temperature needed to be raised can be calculated as Eq. 9.

$$\Delta T_{int} = \frac{Q_{total} \cdot \Delta t}{C_{int}} \tag{9}$$

After ΔT_{int} has been computed, this value is added to the T_{int}, updating the temperature of the interaction node.

3.2 Thermal Haptic Rendering

For thermal haptic rendering, 24 interaction nodes are categorized into 8 *node groups* as shown in Figure 2c. These groups include 'Thumb, Index, Middle, Ring, Pinky, PalmLeft, PalmMiddle, and PalmRight', where each group contains upper, middle, and lower interaction nodes (Figure 4). At first, the temperature of each interaction node is converted to $H_{i,low}, H_{i,mid}$, and $H_{i,up}$ as Eq. 10∼Eq. 12.

$$H_{\text{i,up}} = T_{\text{i,up}} - T_{\text{base}} \tag{10}$$

$$H_{\text{i,mid}} = T_{\text{i,mid}} - T_{\text{base}} \tag{11}$$

$$H_{\text{i,low}} = T_{\text{i,low}} - T_{\text{base}} \tag{12}$$

, where i refers to one of the node groups. T_{base} is the baseline temperature of the interaction nodes, which we set as typical skin temperature (33°C).

$$H_{\text{i}} = max\left(H_{\text{i,low}}, H_{\text{i,mid}}, H_{\text{i,up}}\right) \tag{13}$$

, where H_{i} is *node group*'s highest temperature difference from one of the $H_{\text{i,low}}$, $H_{\text{i,mid}}$, and $H_{\text{i,up}}$.

Thermal Rendering In default, PID's target temperature is set to T_{base} (33°C). If the target temperature gets higher, the system heats the FTED. If the target temperature gets lower, then the system turns the device off for cooling. When all H_i have been computed, the PID controller assigns intensity for each FTED based on the H_{i} as shown in Eq. 14∼ 17. Here, the outputs of the PID are set as either mode 1, 2, or 3.

$$P_{\text{Thumb}} = \text{PID}\left(H_{\text{T}}\right) \tag{14}$$

$$P_{\text{Left}} = \text{PID}\left(max\left(H_{\text{I}}, H_{\text{M}}\right)\right) \tag{15}$$

$$P_{\text{Right}} = \text{PID}\left(max\left(H_{\text{M}}, H_{\text{R}}, H_{\text{P}}\right)\right) \tag{16}$$

$$P_{\text{Palm}} = \text{PID}\left(max\left(H_{\text{PL}}, H_{\text{PM}}, H_{\text{PR}}\right)\right) \tag{17}$$

Tactile Rendering After computing the target temperature for all the interaction nodes, we move on to calculate the LRAs' intensities. For each node group, there exist 2 LRAs and 3 interaction nodes. We compute intensities using Eq. 18∼20.

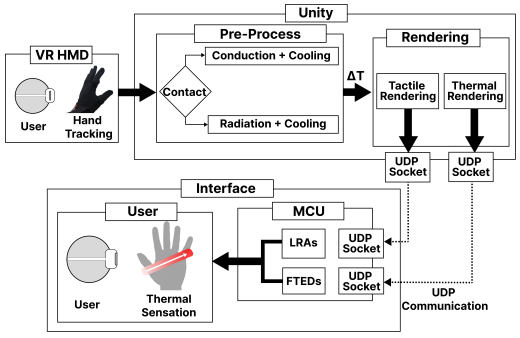

Figure 5: System flow of multimodal thermal rendering.

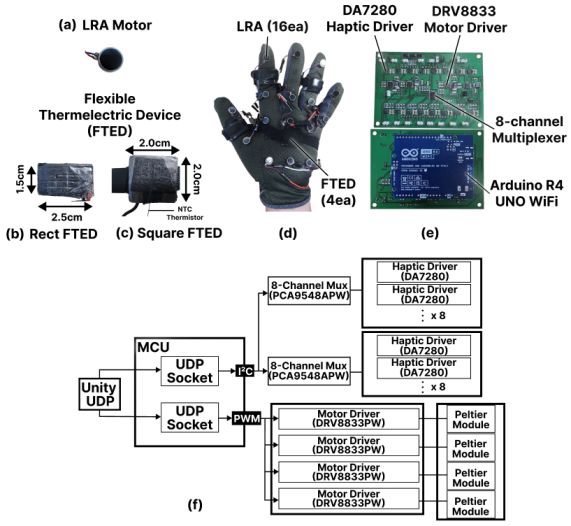

Figure 6: ThermicVib hardware detail. ThermicVib consists of (a) LRAs, flexible thermoelectric devices with (b) rectangular (thumb, index, and ring fingers) and (c) square (palm) shapes with NTC Thermisitor attached. (d) Our prototype contains 16 LRAs and 4 TEDs operated with (e),(f) customized board.

$$w_{grp} = \frac{H_i}{T_{max} - T_{base}} \tag{18}$$

$$R_{i,down} = \log_2\left(1 + \frac{H_{i,low} + 0.5 \cdot H_{i,mid}}{H_{i,low} + H_{i,mid} + H_{i,up}}\right) \cdot w_{grp} \tag{19}$$

$$R_{i,up} = \log_2\left(1 + \frac{H_{i,up} + 0.5 \cdot H_{i,mid}}{H_{i,low} + H_{i,mid} + H_{i,up}}\right) \cdot w_{grp} \tag{20}$$

. $R_{i,down}$ and $R_{i,up}$ refer to the ratio of lower and upper temperature difference that is used to decide the intensity ratio of LRAs. w_{grp} is a weight for adjusting ratios within the node group based on temperature difference. If the difference increases, so does the weight. T_{max} is the highest temperature for the system to render, which we set under pain threshold (45°C).

$R_{i,down}$ and $R_{i,up}$ are ratios that only consider the temperature difference within the node group. For a whole-hand context, temperature differences between groups should also be considered. For example, if the index finger's temperature is higher than that of the middle finger, then LRA intensities for the index finger should be higher

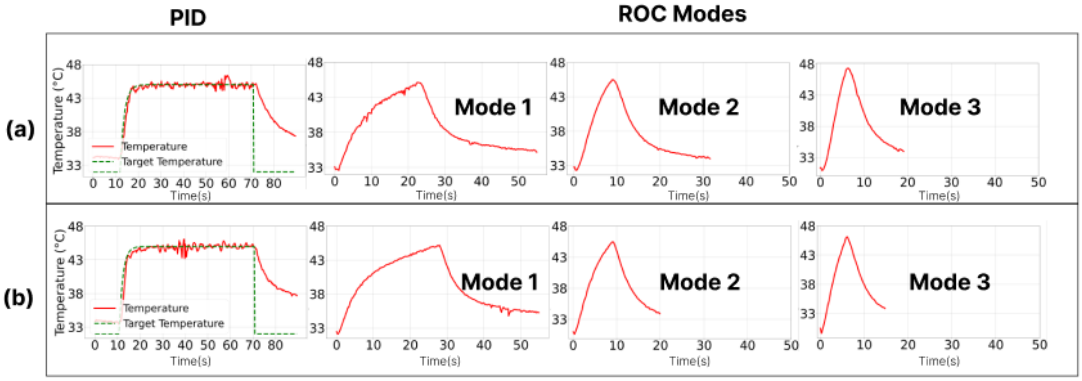

Figure 7: Thermal Device Characterization. (a) is for Rect FTED and (b) is for Square FTED. The left graphs are PID Characterization, and the right graphs are characterization of three modes of ROC. Note that the temperature is the FTED's.

than that for the middle finger. To reflect a whole hand context to the LRAs, a new weight w_{hand} is applied, which is shown in Eq. 21,

$$w_{hand} = \frac{H_i - GH_{min}}{GH_{max} - GH_{min}} \tag{21}$$

, where $GH_{\max}$ is the highest temperature difference value among all the node groups and $GH_{\min}$ is the lowest temperature difference which is shown in Eq. 22 and Eq. 23.

$$GH_{\max} = \max\left(H_{\mathrm{T}}, H_{\mathrm{I}}, H_{\mathrm{M}}, H_{\mathrm{R}}, H_{\mathrm{P}}, H_{\mathrm{PL}}, H_{\mathrm{PM}}, H_{\mathrm{PR}}\right) \tag{22}$$

$$GH_{\min} = \min\left(H_{\mathrm{T}}, H_{\mathrm{I}}, H_{\mathrm{M}}, H_{\mathrm{R}}, H_{\mathrm{P}}, H_{\mathrm{PL}}, H_{\mathrm{PM}}, H_{\mathrm{PR}}\right) \tag{23}$$

After the $R_{i,down}$ and $R_{i,up}$ are calculated, intensity ratios for upper and lower LRA are determined as Eq. 24 and Eq. 25

$$I_{i,up} = R_{i,up} \cdot w_{hand} \cdot I_{max} \tag{24}$$

$$I_{i,down} = R_{i,down} \cdot w_{hand} \cdot I_{max} \tag{25}$$

, where $I_{i,up}$ and $I_{i,down}$ is the upper and lower LRAs' ratios that are adjusted with node group context in range of 0 to I_{max}. I_{max} is the max intensity ratio set in the system. We set the I_{max} to be 0.5 to reduce discomfort [41].

Rendering Integration After all the ratio calculations for both LRAs and FTEDs are done, the system sends signals to the actuators via WiFi UDP communication as shown in Figure 5. Here, the thermal signal is sent 242 ms faster than the tactile signal [21] for better simultaneity. Then, FTEDs and LRAs activate according to the command they received, creating thermal referral and vibrotactile phantom sensation. The system's end-to-end latency was 480ms and computation frequency was 4 Hz.

4 Implementation

4.1 Hardware

We placed a total of 16 LRAs and 4 FTEDs on the glove (Figure 6d). We placed LRAs upper and lower of each node group to enable vibrotactile phantom sensation within a node group. For FTEDs, we left out the middle finger based on the previous studies [10, 14], which showed that users felt a thermal sensation on the middle finger when thermal stimuli were given to the index and ring fingers. Also, we left a pinky finger with no FTED since the Ulnar nerve is shared between the pinky and ring fingers [43]. For other fingers we attached FTED in the middle of them. In this way, the thermal referral covered the whole hand area.

We used two different sizes of FTEDs (Tegway), including rectangular (2cm×2cm) and square (2.5cm×2.5cm) shapes and LRAs with 0.8cm diameter (Figure 6a,b,c). We applied rectangular FTED on the fingers and square FTED on the palm according to the area sizes. We placed TC Thermistor (GA10K3MCD1, TE Connectivity) on the contact side of FTED for temperature control. FTEDs were powered with 5V, 3A maximum, and LRAs with 3V with an average of 0.3A∼0.6A. Figure 6f shows how we controlled LRAs and FTEDs. We employed Arduino R4 WiFi to operate all FTEDs and LRAs through PWM and I^2C accordingly (Figure 6f). Motor drivers (DRV8833, Texas Instruments) were used to control FTEDs with a parallel circuit for higher currents. For control of LRAs, 8-channel multiplexers (PCA9548APW, NXP) and haptic drivers (DA7280, Renesas) were used.

4.2 Thermal Controller

We regulated the temperature of FTED using a PID controller. Figure 7 illustrates the characteristics of the PID controller at an ambient temperature of 25°C. Here, Figure 7a is the PID applied FTED's temperature graph of the rectangular FTED (P=250, I=10, D=100), and Figure 7b is for the square FTED (P=200, I=8, D=80). We maintained the target temperature with no cooling activation of FTED. However, there were noises in both graphs due to the WiFi communication noise in Arduino R4. We observed that the PID controller successfully maintained the temperature for about a minute. We limited the output of PID control to 3 RoC modes (Mode 1,2,3) as shown in Figure 7 for both types of FTED. Three modes are set to follow the ROC of 0.5°C/s, 1.5°C/s, or 2.5°C/s.

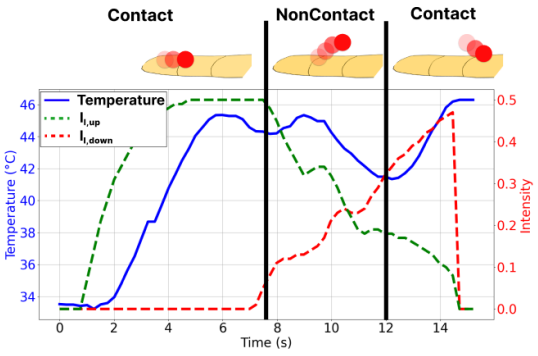

Figure 8: Characteristic of multimodal rendering. The graph shows LRAs' intensities and FTED's temperature change when interacting with a thermal object in both conditions.

4.3 Multimodal Rendering Approach

For the rendering, a virtual thermal object and a virtual hand model were used in a VR scene. Contact and noncontact conditions were based on whether the thermal object was in contact with the virtual hand. When the object moved, the calculation described in Section 3.2 was executed based on the geometric context of the interaction nodes and the object. Then FTEDs and LRAs were activated to create thermal and phantom sensations. With thermal and tactile stimuli present, thermal referral would occur following the phantom sensation. Figure 8 shows the activation characteristics of LRAs and FTEDs in the index node group with contact and noncontact conditions.

5 User Study

To evaluate the proposed interface, we conducted two user studies. In Study 1, we measured the localization accuracy of our rendering on the whole hand during static (point localization) and dynamic sensations (pattern identification). In Study 2, we asked users to interact with a cat and a fire with VR HMD. For Study 2, we confirmed the user experience using our approach. The whole study took less than 2 hours, and we fixed the room temperature to 25°C. For detailed results with the confusion matrices, please refer to supplement materials.

5.1 Study Setup

We recruited 21 participants (mean age: 28.1, SD: 3.7, 13 male, 8 female). None of them had problems with sensing thermal feedback on hand or wearing our gloves.

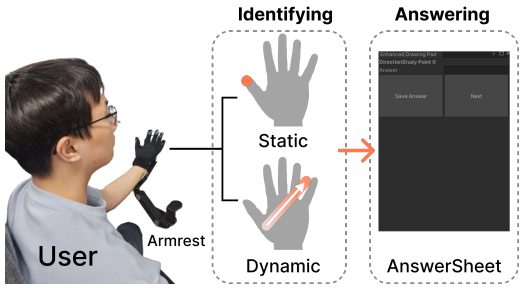

Figure 9: Study 1 setup. We asked a user to identify the static and dynamic thermal sensations on the whole hand.

In Study 1, we shared the same setup for static and dynamic thermal sensations as shown in Figure 9. Each participant wore our multimodal haptic glove on their left hand since there was not much difference between the left and right hand for thermal sensation [34]. Before the experiment, participants sat down and placed their left arm on the armrest fixed to a desk for comfort. We forced users to rest for at least 20 s after each response to cool down the skin to neutral zone (32°C∼34°C). If the cooling took longer than 20 s, we used a fan to cool down.

For Study 2, we asked users to wear VR HMD (Meta Quest Pro) along with our prototype and perform two user interaction tasks in a VR scene. We used the hand tracking supported from the VR HMD to enable to full interactions for the study.

5.2 Study 1: Point Localization and Pattern Recognition

5.2.1 Point Localization

Procedure First, we showed the location of 24 thermal points and provided this visual map to participants. After wearing our glove, an outer cover was worn to the glove to prevent users from assuming answers from the devices'

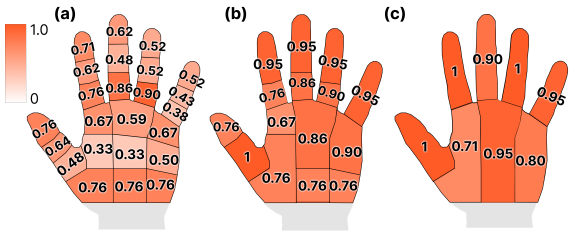

Figure 10: Visualization of thermal points' locations and measured accuracies. (a) is the accuracy of all 24 interaction nodes. (b) is accuracy of newly defined interaction nodes based on the (a)'s result. (c) is the accuracy of node groups.

locations. For each location, the thermal point sensation was given for 8 s with increasing temperature from 33°C to 45°C. Then, users responded with the location number on the visual map to denote the location of the thermal point sensation. Each user carried out 24 trials (24 locations) in a random order without duplicates.

Results Overall average accuracy was 61% (SD=16) to localize the thermal sensation location within 24 interaction nodes (Figure 10a). Palm had low accuracy, including the middle nodes of PL (33%), PR (33%), and lower node of P(38%) as well. In terms of node grouping for thermal sensation, we observed that the accuracy increased to 92% (SD=9) (Figure 10c). We also observed a relatively better performance in the palm area when following the node group for localization. However, the left palm still had relatively low accuracy (71%), which users were often confused with the thumb. We regrouped the most mistaken answers within the group as a new interaction node and measured the accuracy as shown in Figure 10b. The accuracy was an improved average of 85% (SD=9), which shows that thermal points were identifiable in these newly defined nodes.

Overall, for node group resolution, the results show that thermal sensation was well perceived. Also, P, M, PL, and PR group, where phantom sensation was used, the thermal referral was also successfully identified.

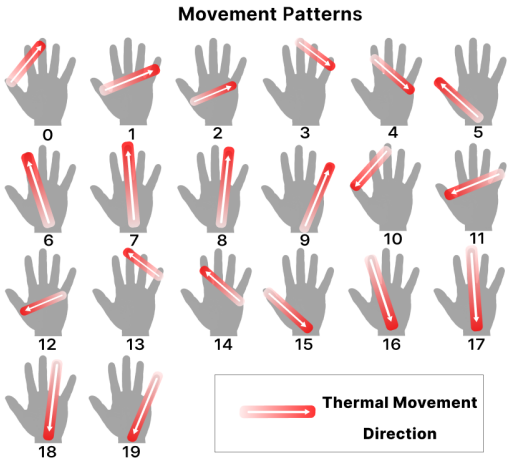

Figure 11: A list of thermal patterns for Study 1.

5.2.2 Pattern Recognition

Procedure We showed 20 dynamic thermal sensation patterns to each participant. We created the dynamic patterns to cover the whole hand in various directions

by connecting 2 interaction nodes at the start and end position (Figure 11). The rendered speed was fixed to 0.8cm/s. Patterns 5∼9 and 15∼19 show dynamic rendering that stayed within the hand, starting from PM to each fingertip and vice versa. Patterns 0∼4 and 10∼14 show dynamic rendering that crossed different groups horizontally. The pattern started after 4 seconds of heating to reach 45°C. Then, the movement was rendered from the start to the end, and we asked users to identify the given patterns. We presented 20 trials in a random order without duplicates (20 patterns). Post-interview was also carried out where participants were asked to rate their perception of thermal movement sensation on a 7-point Likert Scale, with 1 indicating no thermal movement, and 7 indicating a clear sensation. We also asked participants to report if they felt no thermal movement to check the device's operation.

Results The post-interview result showed an average rating of 6.05(SD=0.94), with no one reporting absence of thermal movement sensation, showing that the thermal movement was present during study. The average accuracy was 80% (SD=13), indicating that users were capable of identifying the thermal movement on hand. For patterns on hand (0∼4 and 10∼14) vertically, the average accuracy was 78% (SD=16). For those who crossed different groups horizontally (5∼9 and 15∼19), the mean accuracy was 83% (SD=14), which was higher than vertical direction sensation. Three patterns (2,4,19) had the lowest accuracy of 52%. Thermal pattern 2 was mostly mistaken with 15, 4 with 16, and 19 with 11, which indicates that participants responded to the perceived movement. Overall, the results show that dynamic thermal movement was well perceived.

5.3 Study 2: User Experience Evaluation in VR Scenes

Procedure In this study, the user equipped VR HMD, and we calibrated the study boundary and environment to offer the same experience to every user. We asked for two tasks: 1) Pet different surfaces of the cat with the hand and 2) feel the fire from a distance. Users experienced each task for at least 1 minute. We set the cat's face temperature as 42°C and other body parts as 37°C, so the user felt the temperature difference when touching different body parts. Next, we asked the user to light up the fire and feel the thermal sensation at a distance. The fire was set to 800°C, and we asked users to change the distance minimum of 2 m from the fire and move their hands in various directions around the fire. The maximum temperature of FTED was set to 50°C for the fire experiment. We set two thermal sensation conditions, including 1) thermal-only rendering and 2) multimodal rendering (thermal and vibrotactile rendering). This confirms the user experience in both operating conditions.

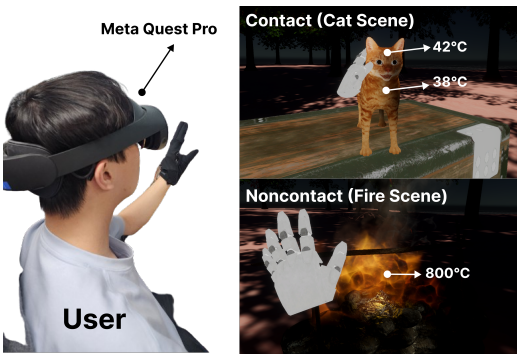

Figure 12: Study 2 Setup. The user wears a VR HMD and experiences the VR scene with various contact conditions.

After completing the task, users responded to questionnaires on *Sensory Fidelity* (13,16,17), *Immersion* (9,21,30), *Involvement* (2,3), *Interface Quality* (19) from the 4-factor presence questionnaire [48]. We also added *Experience* question to see how the thermal sensation was rendered on the whole hand. Table 1 lists all questions for our study. All the questions were answered on a 7-point Likert scale, where a higher number refers to a positive response except for *Interface Quality*, where a lower number (felt no delay) is a positive response. Also, we asked which task they preferred between contact (cat) and noncontact (fire) conditions.

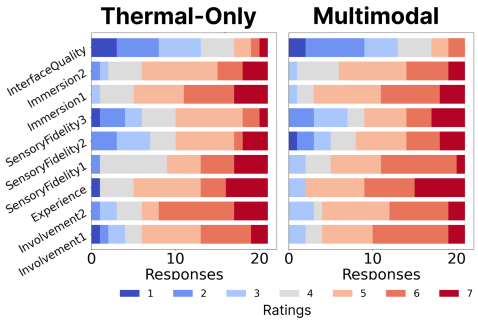

Figure 13: User responses to our questionnaire.

Results Figure 13 shows the result of users with thermal-only and multimodal rendering. One-way ANOVA test and t-tests showed no significant difference between the two conditions ($p > 0.2$ for all metrics). Still, Table 2 shows that multimodal rendering was slightly better in every metric. In one question, Involvement 2, Thermal-Only was higher than Multimodal (T: 5.33, M: 5.19). For *Preference*, fire was preferred in both Thermal-Only and Multimodal. However, in Multimodal, the cat's preference increased compared to Thermal-Only. The overall result shows that multimodal rendering did improve the user experience, especially the Experience result shows that thermal sensation on the whole hand was well perceived.

6 Discussion

Results from point localization show that our interface supported static and dynamic thermal sensation. Figure 10c indicates that the node group was well defined and multimodal rendering was well perceived from the node group point of view. From Figure 10a, we assumed that although thermal referral was created, the perceived area was larger than the interaction nodes. Figure 10b, shows what interaction nodes were perceived as one node. This also indicates that our rendering approach was effective since users could distinguish the thermal sensation's location on the hand.

Pattern recognition results show that our multimodal approach successfully rendered thermal movement on the whole hand. For the 3 patterns that scored the lowest accuracy, we assumed that this was due to the space between the hand and glove textile surface, which reduces the thermal sensation transfer to the skin. For future work, the glove's fit to the user's hand should be guaranteed to provide an effective thermal sensation. An interesting thing to note is that patterns 0 and 10, which moved out of hand, had high accuracy of 90% and 95%. This indicates that thermal referral could get triggered by out-of-hand vibrotactile phantom sensation.

Table 1: Evaluation categories and questionnaires.

Category	Questions
Involvement	1. How responsive was the environment to actions that you initiated (or performed)? 2. How naturally did your interactions with the objects seem?
Experience	1. Were thermal sensations well perceived on hand overall?
Sensory Fidelity	1. Did the thermal sensation change well based on distance with the thermal object? 2. Did the thermal sensation change well based on the direction of the hand to the fire? 3. Did thermal sensation change well according to the contact?
Immersion	1. Were there moments when you felt completely focused on the task/environment in VR? 2. Were you able to anticipate what would happen next in response to the actions that you performed?
Interface Quality	1. How much delay did you experience between your actions and expected outcomes?
Preference	1. Which interaction did you prefer? The cat or the fire?

Table 2: Mean and Standard Deviations for Questionnaire Results

Metric	Thermal-Only	Multimodal
Involvement	5.10 (1.41)	5.26 (1.04)
Experience	5.24 (1.45)	5.67 (1.20)
SensoryFidelity	4.54 (1.27)	4.82 (1.35)
Immersion	5.19 (1.04)	5.26 (0.87)
InterfaceQuality	3.19 (1.63)	3.14 (1.49)

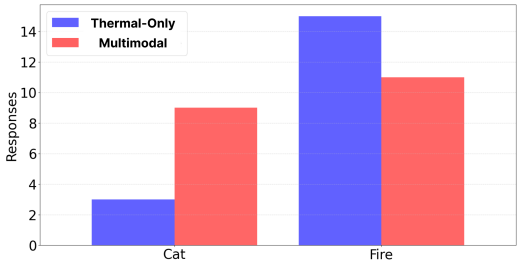

Figure 14: Contact (Cat) and noncontact (fire) preference.

Study 2 results show that our multimodal approach showed a similar or slightly better overall experience than the thermal-only approach. We assume that this might be caused by thermal referral sensation by activating multiple FTEDs. We found out that we enabled thermal referral in thermal-only conditions as well since our rendering algorithm created the phenomenon with the temperature change of FTEDs. Thus, not much sensation difference might happen even with multimodal rendering in this case. The high scores on every metric (> 4.5 on average) for both thermal-only and multimodal rendering still tell the high quality of thermal sensation experience using the ThermicVib prototype.

Our finding on the user preference for various contact conditions tells us that we could increase the user experience by appropriately rendering thermal sensation based on the contexts. As shown in Figure 14, vibration degraded the noncontact condition (fire) experience since users did not expect much vibrotactile feedback in this condition. However, *Preference* for contact condition (cat) increased, which suggests that our suggested multimodal rendering is more applicable for thermal interaction that includes tactile experience (e.g., touching). For fire still being preferred over the cat in multimodal rendering, we assumed that the cat visual affected the user, expecting the cat's softness to be applied to the vibration, which was not our scope of rendering. To improve our interface, utilizing thermal-only rendering for noncontact situations and multimodal rendering for contact may need to be considered in future work. As shown in the Study 1 results, the number of interaction nodes in our interface was sufficient to represent maximum spatial resolution for our rendering while maintaining acceptable perceptual performance. However, the spatial resolution of our approach can be limited by other factors, such as the performance and size of the vibrotactile and thermal actuators.

Also, to fully render thermal sensation, the cold sensation should be considered in the future. The cold sensation was excluded in our work to maintain a minimal wearable physical form factor for broad acceptance. The activation of cooling often requires an external heat sink due to low heat dissipation. If generated heat from FTED is not efficiently removed, it can eventually increase the temperature, degrading the cooling effect. Previous works [15, 49] added tubes and fans to quickly dissipate the heat, which increases the overall size of the form factor. We plan to apply a suitable heat sink for our form factor in the future. Another FTED's limitation was that the ROC was hard to be stabled, which needs to be further studied as well. In this work, we focused on the combined effect of phantom sensation and thermal referral to explore the potential of introducing a thermal movement experience. Although explicit quantitative studies would be required to determine the detailed parameters to enhance the thermal movement sensation, we have shown that our approach enabled new thermal sensations and experiences.

7 Conclusion

In this study, we proposed a multimodal haptic glove with integrated sensory illusions for dynamic thermal sensation. With our interface, we enabled both static and dynamic thermal sensations on the whole hand, considering various heat conditions. Results also suggest that ThermicVib has the potential to enhance the user experience when interacting with virtual objects, as our interface renders active perception of thermal sensation. We hope that our approach extends the modality of haptic interaction to bring rich and immersive experiences to users.

Supplemental Materials

There are supplemental materials available containing confusion matrices for Study 1 results.

Acknowledgments

This research is supported by Ministry of Culture, Sports and Tourism(MCST) and Korea Creative Content Agency(KOCCA) in the Culture Technology(CT) Research Development Program 2023 (No.00216939) and Electronics and Telecommunications Research Institute(ETRI) grant funded by the Korean government [24ZC1200, Research on hyper-realistic interaction technology for five senses and emotional experience].

References

[1] D. S. Alles. Information transmission by phantom sensations. *IEEE transactions on man-machine systems*, 11(1):85–91, 1970. 1, 2

[2] T. L. Bergman. *Fundamentals of heat and mass transfer*. John Wiley & Sons, 2011. 3

[3] J. C. STEVENS KENNETH K. CHOO. Temperature sensitivity of the body surface over the life span. *Somatosensory & motor research*, 15(1):13–28, 1998. doi: 10.1080/08990229870925 2

[4] S. Cai, P. Ke, T. Narumi, and K. Zhu. Thermairglove: A pneumatic glove for thermal perception and material identification in virtual reality. In *2020 IEEE conference on virtual reality and 3D user interfaces (VR)*, pp. 248–257. IEEE, 2020. doi: 10.1109/VR46266.2020.00044 2

[5] A. Cataldo, E. R. Ferrè, G. Di Pellegrino, and P. Haggard. Thermal referral: evidence for a thermoceptive uniformity illusion without touch. *Scientific reports*, 6(1):35286, 2016. doi: 10.1038/srep35286 1, 2

[6] J. Dionisio, V. Henrich, U. Jakob, A. Rettig, and R. Ziegler. The virtual touch: Haptic interfaces in virtual environments. *Computers Graphics*, 21(4):459–468, 1997. Haptic Displays in Virtual Environments and Computer Graphics in Korea. doi: 10.1016/S0097-8493(97)00029-0 1

[7] P. O. Fanger. *Thermal comfort. Analysis and applications in environmental engineering.* Copenhagen: Danish Technical Press. 3

[8] A. J. Fay and J. K. Maner. Warmth, spatial proximity, and social attachment: The embodied perception of a social metaphor. *Journal of Experimental Social Psychology*, 48(6):1369–1372, 2012. doi: 10.1016/j.jesp.2012.05.017 1

[9] F. A. Geldard and C. E. Sherrick. The cutaneous" rabbit": a perceptual illusion. *Science*, 178(4057):178–179, 1972. doi: 10.1126/science.178.4057.178 2

[10] B. G. Green. Localization of thermal sensation: An illusion and synthetic heat. *Perception & Psychophysics*, 22(4):331–337, 1977. doi: 10.3758/BF03199698 2, 5

[11] S. Günther, F. Müller, D. Schön, O. Elmoghazy, M. Mühlhäuser, and M. Schmitz. Therminator: Understanding the interdependency of visual and on-body thermal feedback in virtual reality. In *Proceedings of the 2020 CHI Conference on Human Factors in Computing Systems*, pp. 1–14, 2020. doi: 10.1145/3313831.3376195 2

[12] M. Halvey, G. Wilson, Y. Vazquez-Alvarez, S. A. Brewster, and S. A. Hughes. The effect of clothing on thermal feedback perception. In *Proceedings of the 13th international conference on multimodal interfaces*, pp. 217–220, 2011. doi: 10.1145/2070481.2070519 2

[13] H.-N. Ho, J. Watanabe, H. Ando, and M. Kashino. Somatotopic or spatiotopic? frame of reference for localizing thermal sensations under thermo-tactile interactions. *Attention, Perception, & Psychophysics*, 72:1666–1675, 2010. doi: 10.3758/APP.72.6.1666 2

[14] H.-N. Ho, J. Watanabe, H. Ando, and M. Kashino. Mechanisms underlying referral of thermal sensations to sites of tactile stimulation. *Journal of Neuroscience*, 31(1):208–213, 2011. doi: 10.1523/JNEUROSCI.2640-10.2011 2, 5

[15] P. P. Hoffmann, H. Elsayed, M. Mühlhäuser, R. R. Wehbe, and M. D. Barrera Machuca. Thermalpen: Adding thermal haptic feedback to 3d sketching. In *Extended Abstracts of the 2023 CHI Conference on Human Factors in Computing Systems*, pp. 1–4, 2023. doi: 10.1145/3544549.3583901 2, 8

[16] J. P. Holman. *Heat transfer*. McGraw Hill, 1986. 3

[17] J. Hua, M. Furukawa, and T. Maeda. Extrapolation of thermal sensation: Warm-cold stimulus pair elicits a sense of warmth outside the stimulus. *Authorea Preprints*, 2024. doi: 10.36227/techrxiv.171043149.92624860/v1 2

[18] Y. Huang, K. Yao, J. Li, D. Li, H. Jia, Y. Liu, C. K. Yiu, W. Park, and X. Yu. Recent advances in multi-mode haptic feedback technologies towards wearable interfaces. *Materials Today Physics*, 22:100602, 2022. doi: 10.1016/j.mtphys.2021.100602 1

[19] A. Israr and I. Poupyrev. Control space of apparent haptic motion. In *2011 IEEE world haptics conference*, pp. 457–462. IEEE, 2011. 2

[20] I. Jalilvand, J. Jang, B. Gopaluni, and A. S. Milani. Vr/mr systems integrated with heat transfer simulation for training of thermoforming: A multicriteria decision-making user study. *Journal of Manufacturing Systems*, 72:338–359, 2024. doi: 10.1016/j.jmsy.2023.11.007 2

[21] T. Jodai, M. Terao, L. A. Jones, and H.-N. Ho. Determination of the thermal-tactile simultaneity window for multisensory cutaneous displays*. In *2023 IEEE World Haptics Conference (WHC)*, pp. 230–236, 2023. doi: 10.1109/WHC56415.2023.10224482 5

[22] L. A. Jones and H.-N. Ho. Warm or cool, large or small? the challenge of thermal displays. *IEEE Transactions on Haptics*, 1(1):53–70, 2008. doi: 10.1109/TOH.2008.2 2

[23] J. W. Kelly, L. A. Cherep, B. Klesel, Z. D. Siegel, and S. George. Comparison of two methods for improving distance perception in virtual reality. *ACM Transactions on Applied Perception (TAP)*, 15(2):1–11, 2018. doi: 10.1145/3165285 2

[24] S.-W. Kim, S. H. Kim, C. S. Kim, K. Yi, J.-S. Kim, B. J. Cho, and Y. Cha. Thermal display glove for interacting with virtual reality. *Scientific reports*, 10(1):11403, 2020. 1

[25] S. Kratz and A. Dunnigan. Thermotouch: Design of a high dynamic temperature range thermal haptic display. In *Proceedings of the 2016 CHI Conference Extended Abstracts on Human Factors in Computing Systems*, CHI EA '16, p. 1577–1582. Association for Computing Machinery, New York, NY, USA, 2016. doi: 10.1145/2851581.2892554 2

[26] K. Kushiyama, T. Baba, K. Doi, and S. Sasada. Thermal design display device to use the thermal tactile illusions: " thermo-paradox". In *ACM SIGGRAPH 2010 Posters*, pp. 1–1. 2010. doi: 10.1145/1836845.1836951 2

[27] J. Lee, Y. Kim, and G. J. Kim. Applying "out of body" vibrotactile illusion to two-finger interaction for perception of object dynamics. In *Human-Computer Interaction–INTERACT 2015: 15th IFIP TC 13 International Conference, Bamberg, Germany, September 14-18, 2015, Proceedings, Part IV 15*, pp. 506–509. Springer, 2015. doi: 10.1007/978-3-319-22723-8_49 2

[28] Y. Liu, S. Nishikawa, Y. A. Seong, R. Niiyama, and Y. Kuniyoshi. Thermocaress: A wearable haptic device with illusory moving thermal stimulation. In *Proceedings of the 2021 CHI Conference on Human Factors in Computing Systems*, pp. 1–12, 2021. doi: 10.1145/3411764.3445777 1, 2

[29] H. Luo, Z. Wang, Z. Wang, Y. Zhang, and D. Wang. Perceptual localization performance of the whole hand vibrotactile funneling illusion. *IEEE Transactions on Haptics*, 2023. 1, 2, 3

[30] L. E. Marks and J. C. Stevens. Perceived warmth and skin temperature as functions of the duration and level of thermal irradiation! *Perception & Psychophysics*, 4(4):220–228, 1968. doi: doi.org/10.3758/BF03206306 2

[31] A. McBride, S. Bargmann, D. Pond, and G. Limbert. Thermoelastic modelling of the skin at finite deformations. *Journal of thermal biology*, 62:201–209, 2016. doi: 10.1016/j.jtherbio.2016.06.017 3

[32] T. Morita, Y. Kuwajima, A. Minaminosono, S. Maeda, and Y. Kakehi. Hydromod: Constructive modules for prototyping hydraulic physical interfaces. In *Proceedings of the 2022 CHI Conference on Human Factors in Computing Systems*, pp. 1–14, 2022. doi: 10.1145/3491102.3502096 2

[33] A. Nasser, K.-N. Keng, and K. Zhu. Thermalcane: Exploring thermotactile directional cues on cane-grip for non-visual navigation. In *Proceedings of the 22nd international ACM SIGACCESS conference on computers and accessibility*, pp. 1–12, 2020. doi: 10.1145/3373625.3417004 2

[34] T. Nilsson, L. Burström, M. Hagberg, and R. Lundström. Thermal perception thresholds among young adults exposed to hand-transmitted vibration. *International archives of occupational and environmental health*, 81:519–33, 05 2008.

doi: 10.1007/s00420-007-0258-0 6

[35] R. L. Peiris, W. Peng, Z. Chen, and K. Minamizawa. Exploration of cuing methods for localization of spatial cues using thermal haptic feedback on the forehead. In *2017 IEEE World Haptics Conference (WHC)*, pp. 400–405. IEEE, 2017. doi: 10.1109/WHC.2017.7989935 1

[36] W. Peng, R. L. Peiris, and K. Minamizawa. Exploring of simulating passing through feeling on the wrist: using thermal feedback. In *Adjunct Proceedings of the 30th Annual ACM Symposium on User Interface Software and Technology*, pp. 187–188, 2017. doi: 10.1145/3131785.3131819 2

[37] P. J. Rodríguez de Rivera, M. Rodríguez de Rivera, F. Socorro, M. Rodríguez de Rivera, and G. M. Callicó. A method to determine human skin heat capacity using a non-invasive calorimetric sensor. *Sensors*, 20(12), 2020. doi: 10.3390/s20123431 3

[38] G. Saiko. Skin temperature: The impact of perfusion, epidermis thickness, and skin wetness. *Applied Sciences*, 12(14), 2022. doi: 10.3390/app12147106 3

[39] A. Singhal and L. A. Jones. Perceptual interactions in thermo-tactile displays. In *2017 IEEE World Haptics Conference (WHC)*, pp. 90–95, 2017. doi: 10.1109/WHC.2017.7989882 2

[40] Y. Singhal, H. Wang, H. Gil, and J. R. Kim. Mid-air thermo-tactile feedback using ultrasound haptic display. In *Proceedings of the 27th ACM Symposium on Virtual Reality Software and Technology*, VRST '21. Association for Computing Machinery, New York, NY, USA, 2021. doi: 10.1145/3489849.3489889 1, 2

[41] H. Son, H. Wang, Y. Singhal, and J. R. Kim. Upper body thermal referral and tactile masking for localized feedback. *IEEE Transactions on Visualization and Computer Graphics*, 29(5):2211–2219, 2023. doi: 10.1109/TVCG.2023.3247068 1, 2, 5

[42] Y. Sung, R. Kim, K. W. Song, Y. Shao, and S. H. Yoon. Hapticpilot: Authoring in-situ hand posture-adaptive vibrotactile feedback for virtual reality. *Proceedings of the ACM on Interactive, Mobile, Wearable and Ubiquitous Technologies*, 7(4):1–28, 2024. 1, 2

[43] R. Wakolbinger, A. D. Roche, T. Stockinger, B. Gustorff, and O. C. Aszmann. Multiregion thermal sensitivity mapping of the hand. *Journal of Plastic, Reconstructive & Aesthetic Surgery*, 67(11):1541–1547, 2014. 5

[44] H. Wang, Y. Singhal, H. Gil, and J. Y. Kim. Thermal masking: When the illusion takes over the real. In *Proceedings of the 2024 CHI conference on human factors in computing systems*, 2024. 1

[45] L. E. Williams and J. A. Bargh. Experiencing physical warmth promotes interpersonal warmth. *Science*, 322(5901):606–607, 2008. doi: 10.1126/science.1162548 1

[46] G. Wilson, S. Brewster, M. Halvey, and S. Hughes. Thermal icons: evaluating structured thermal feedback for mobile interaction. In *Proceedings of the 14th international conference on Human-computer interaction with mobile devices and services*, pp. 309–312, 2012. doi: 10.1145/2371574.2371621 2

[47] G. Wilson, M. Halvey, S. A. Brewster, and S. A. Hughes. Some like it hot: thermal feedback for mobile devices. In *Proceedings of the SIGCHI Conference on Human Factors in Computing Systems*, pp. 2555–2564, 2011. doi: 10.1145/1978942.1979316 2

[48] B. G. Witmer, C. J. Jerome, and M. J. Singer. The factor structure of the presence questionnaire. *Presence: Teleoperators & Virtual Environments*, 14(3):298–312, 2005. 7

[49] B. Zhang and M. Sra. Pneumod: A modular haptic device with localized pressure and thermal feedback. In *Proceedings of the 27th ACM Symposium on Virtual Reality Software and Technology*, pp. 1–7, 2021. doi: 10.1145/3489849.3489857 2, 8

[50] Y. Zhou, H. Yu, S. Xu, M. Luo, and X. Zhou. High-density thermal sensitivity of the hand under different thermal states and stimulus intensities. *Indoor air*, 32(8):e13089, 2022. doi: 10.1111/ina.13089 2